BIOCHEMICAL PHARMACOLOGY 75 (2008) 1416–1425

available at www.sciencedirect.com

ScienceDirect

journal homepage: www.elsevier.com/locate/biochempharm

Structure–activity relationship of coumarin derivatives on xanthine oxidase-inhibiting and free radical-scavenging activities

Hsiu-Chen Lin [a,c], *Shin-Hui Tsai* [d], *Chien-Shu Chen* [e], *Yuan-Ching Chang* [f,g], *Chi-Ming Lee* [d], *Zhi-Yang Lai* [b,c], *Chun-Mao Lin* [c,d,*]

[a] *Department of Laboratory Medicine, Taipei Medical University Hospital, Taipei, Taiwan*
[b] *Department of Internal Medicine, Taipei Medical University Hospital, Taipei, Taiwan*
[c] *School of Medicine, Taipei Medical University, Taipei, Taiwan*
[d] *Graduated Institute of Medical Sciences, Taipei Medical University, Taipei, Taiwan*
[e] *School of Pharmacy, College of Medicine, National Taiwan University, Taipei, Taiwan*
[f] *Department of General Surgery, Mackay Memorial Hospital, Taipei, Taiwan*
[g] *Mackay Medicine, Nursing and Management College, Beitou, Taipei, Taiwan*

ARTICLE INFO

Article history:
Received 19 September 2007
Accepted 27 November 2007

Keywords:
Coumarin
Esculetin
Molecular modeling
ROS
Xanthine oxidase

ABSTRACT

We employed 1,1-diphenyl-2-picrylhydrazyl hydrate (DPPH)– and 5,5-dimethyl-1-pyrroline-*N*-oxide (DMPO)–electron spin resonance (ESR) to study the effects of suppression of reactive oxygen species (ROS) by eight selected coumarin derivatives under oxidative conditions. Esculetin was the most potent radical scavenger among the eight tested compounds. Our results suggest that the number of hydroxyl groups on the ring structure of coumarins is correlated with the effects of ROS suppression. We also investigated the effect of the derivatives on the inhibition of xanthine oxidase (XO) activity, and the structure–activity relationships (SARs) of these derivatives against XO activity were further examined using computer-aided molecular modeling. All determined derivatives competitively inhibited XO. The results of the structure-based molecular modeling exhibited interactions between coumarins and the molybdopterin region of XO. The carbonyl pointed toward the Arg880, and the ester O atom formed hydrogen bonds with Thr1010. Esculetin, which bears two hydroxyl moieties on its benzene rings, had the highest affinity toward the binding site of XO, and this was mainly due to the interaction of 6-hydroxyl with the E802 residue of XO. The hypoxanthine/XO reaction in the DMPO-ESR technique was used to assess the combined effect on enzyme inhibition and ROS suppression by these coumarins, and the results showed that esculetin was the most potent agent among the tested compounds. We further evaluated the effects of the test compounds on living cells, and esculetin was still the most potent agent at protecting cells against ROS-mediated Aβ-damage among the tested coumarins.

* *Corresponding author at*: College of Medicine, Taipei Medical University, 250 Wu-Hsing Street, Taipei 110, Taiwan. Tel.: +886 2 27361661x3165; fax: +886 2 27387348.
E-mail address: cmlin@tmu.edu.tw (C.-M. Lin).
0006-2952/$ – see front matter
doi:10.1016/j.bcp.2007.11.023

1. Introduction

A redox imbalance in a healthy living system leads to malfunctioning of cells that ultimately results in various diseases, including cancer, neurological degeneration, and arthritis as well as accelerating the aging process. These consequences become even more harmful when genetic variations impair the normal degradation of these altered proteins. Therefore, therapeutic strategies should aim at reducing free-radical formation and scavenging free radicals [1]. The toxicity ascribed to the superoxide radical is believed to be caused by superoxide's direct interaction with biological targets. Reactive oxygen species (ROS) can initiate a wide range of toxic oxidative reactions [2]. ROS released by phagocytic cells are involved in the link between inflammation and cancer. Excessive and persistent formation of ROS by inflammatory cells is thought to be a key factor in their genotoxic effects. Intracellular ROS production is associated with a number of cellular events including activation of NAD(P)H oxidase, xanthine oxidase (XO), and the cellular mitochondrial respiratory chain [3].

XO is an important source of free radicals and has been reported in various physiological and pathological models. XO causes gout and is responsible for oxidative damage to living tissues. This enzyme reduces molecular oxygen, leading to the formation of $O_2^{\bullet -}$ and hydrogen peroxide. Regulation of XO activity is important during inflammation [4]. Treatment with an XO inhibitor largely prevented the development of endothelial dysfunction and atherosclerosis in mice [5]. XO catalyses the oxidation of hypoxanthine and xanthine to uric acid yielding superoxide radicals and raises the oxidative level in an organism. Hydroxylation takes place at the molybdopterin center (Mo-pt) via an Mo–OH oxygen which forms a bond with a carbon atom of the substrate such that the oxygen atom is derived from water rather than molecular oxygen [6]. The active form of XO is as a homodimer with a molecular weight of 290 kDa, with each of the monomers acting independently during catalysis. Each subunit contains one molybdopterin cofactor, two distinct [2Fe–2S] centers, and one FAD cofactor. The co-crystal structure of salicylate–XO was first reported by Enroth et al. [7] and was provided for structure-based docking studies.

Natural polyphenols can be divided into several different classes depending on their basic chemical structure which ranges from simple molecules to highly polymerized compounds. Coumarin (known as 1,2-benzopyrone), consisting of fused benzene and α-pyrone rings, is an important group of low-molecular weight phenolics [8] and has been widely used for the prevention and treatment of venous thromboembolism, myocardial infarction and strokes [9]. Coumarins acting to inhibit XO inhibition have been reported [10]. The structure–activity relationships (SARs) of coumarins interacting with this enzyme have also been discussed [11,12]. However, the influences of enzyme–substrate binding by coumarins and the stereochemistry on XO have not been characterized. In this study, the protective effect of some coumarins against ROS and their influence on binding to the active site of XO by various substitution groups and positions on coumarins were investigated. We also combined the ROS-scavenging and XO-inhibition roles of coumarins in order to identify which compounds are more vital to therapeutic applications. We eventually applied our results to living cells to confirm the conclusions drawn from the *in vitro* experiments.

2. Materials and methods

2.1. Materials

Coumarin, 4-hydroxycoumarin, 7-hydroxycoumarin, esculetin, scopoletin, dihydrocoumarin, 4-methylesculetin, and 7-hydroxy-4-methylcoumarin were purchased from ACROS (Geel, Belgium) (Fig. 1). XO (XO, EC 1.2.3.2.), xanthine, and allopurinol were purchased from Sigma (St. Louis, MO). All of the solvents used in this study were from E. Merck (Darmstadt, Germany). Minimum essential medium (MEM), fetal bovine serum (FBS), penicillin, and streptomycin were obtained from Gibco BRL (Grand Island, NY). β-Amyloid peptide ($A\beta_{25-35}$ fragment) was purchased from Jerini Peptide Technologies (Berlin, Germany).

2.2. Cell culture

Neuro-2A neuroblastoma cells (BCRC 60026) were purchased from CCRC (Culture Collection and Research Center, Hsinchu, Taiwan). Cells were grown in MEM containing 10% FBS, 1% nonessential amino acid, and 100 μg/ml penicillin–streptomycin. Conditions were maintained in humidified 95% air/5% CO_2 incubator at 37 °C.

2.3. DPPH radical-scavenging assay

The reaction was performed in 3 ml of methanol containing 250 μM of freshly prepared 1,1-diphenyl-2-picrylhydrazyl hydrate (DPPH). The reaction mixtures were protected from light and incubated for 90 min at room temperature, after which the absorbance of the remaining DPPH was determined colorimetrically at 517 nm. The scavenging activities of coumarins (100 μM) were measured as the decrease in absorbance of DPPH expressed as a percentage of the absorbance of a control DPPH solution without coumarins [13].

2.4. XO activity assay

The enzyme activity was measured spectrophotometrically by continuously measuring uric acid formation at 295 nm with xanthine as the substrate. The XO assay consisted of a 500-μl reaction mixture containing 7.5 mM phosphate buffer, 20 mM 3-(cyclohexylamino)-1-propanesulfonic acid (CAPS), 38 μM EDTA (pH 7.0), 3 U/l XO, and 50 μM xanthine as the substrate. The assay was initiated by adding the enzyme to the reaction mixture without or with inhibitors. The assay mixture was incubated for 3 min at 37 °C, and absorbency readings were taken every 5 s [14]. The extent of inhibition was expressed as the chemical concentration required to inhibit 50% of the enzyme activity (IC_{50}). The inhibition type was determined by the Lineweaver–Burk plot. The substrate concentrations were 20, 40, and 60 μM, respectively, in the reaction mixture without or with inhibitors. All data obtained from the enzyme assays

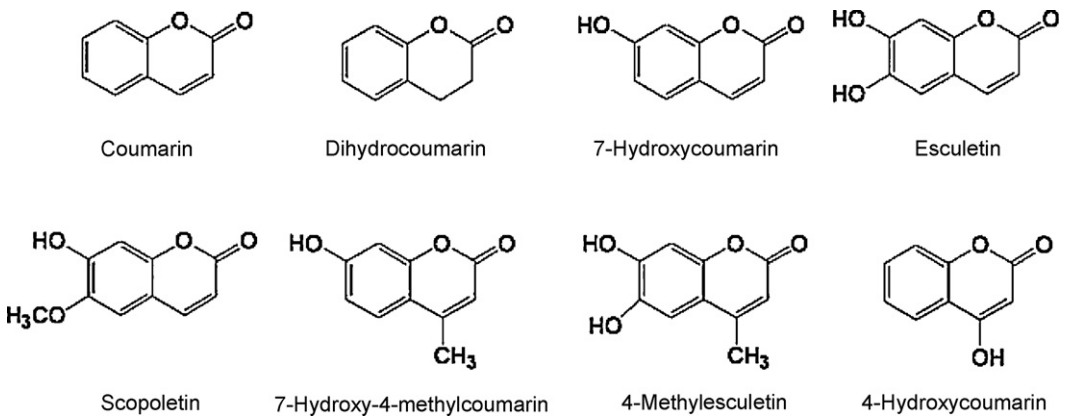

Fig. 1 – Chemical structures of the coumarin derivatives.

and plotting was carried using Excel (Microsoft Office 2003, Microsoft, Taiwan).

2.5. *Computational molecular docking*

To explore the probable binding interactions of the inhibitors with XO, we performed molecular modeling studies using the docking program AutoDock (vers. 3.0) [15]. AutoDock can dock conformationally flexible ligands into a protein, while keeping the protein fixed. The X-ray crystal structure of bovine XO in a complex with salicylate (PDB ID code 1FIQ, Protein Data Bank: http://www.rcsb.org/pdb) [7] was used for the docking studies. The A- and B-chains of the protein and all small molecules were removed except for the two structural waters, Wat176 and Wat196, at the active site. The Wat176 water molecule was found to be H-bonded to the carboxylate group of salicylate. In addition, an oxygen atom single-bonded to the Mo ion was replaced with a water molecule to mimic the water supply during enzyme catalysis. After adding polar hydrogens, the protein atoms were assigned Kollman united-atom partial charges. The 3D structures of the inhibitor molecules were built and optimized by energy minimization using the Tripos force field in the software package SYBYL 6.5 (Tripos, St. Louis, MO). The partial atomic charges were calculated using the Gasteiger–Marsili method [16]. Rotatable bonds in the ligands were assigned with AutoTors implemented in the AutoDock program. To carry out docking simulations, a grid box was defined to enclose the active site with dimensions of 22.5 Å × 22.5 Å × 22.5 Å and a grid spacing of 0.375 Å. The grid maps for energy scoring were calculated using AutoGrid. Docking calculations were performed using the Lamarckian genetic algorithm (LGA) and the pseudo-Solis and Wets local search method. Default parameters were used except for the maximum number of energy evaluations (1×10^6) and docking runs (100). From the docking results, the best-scoring (i.e., with the lowest docking energy) docked model of a compound was chosen to represent its most favorable binding mode predicted by AutoDock. In the present study, all computer simulations were performed on a Silicon Graphics Octane workstation (R12000 270-MHz dual processor) or a Silicon Graphics O_2 workstation (R5000 180-MHz single processor).

2.6. *ESR trapping assay*

Inhibition of iron-induced $^{\bullet}OH$ formation was determined using the ESR trapping technique in combination with 5,5-dimethyl-1-pyrroline-*N*-oxide (DMPO). The signal intensity of DMPO–OH (an adduct of DMPO and a hydroxyl radical) was obtained from the Fenton reaction system containing 60 mM DMPO, 2 mM H_2O_2, and 50 μM ferrous ammonium sulfate with (20, 50, and 100 μM, respectively) or without the test coumarins. This mixture was transferred to a flat quartz cell, and the ESR spectrum was measured 40 s after the addition of ferrous ammonium sulfate. The signals generated in the reaction system were detected using a Bruker ER070 spectrometer (Karlsruhe, Germany) at room temperature [17]. The intensity of the DMPO–OH spin adduct was evaluated by comparing the peak height of the signal. Instrumental conditions were as follows: a central magnetic field of 3475 G, an X-band modulation frequency of 100 kHz, power of 6.4 mW, a modulation amplitude of 5 G, a time constant of 655.4 ms, and a sweep time of 83.9 s. ESR spectra were measured at room temperature.

Combined ROS-scavenging and XO-inhibition activities were measured using the DMPO spin adduct generated in the hypoxanthine (HPX) and XO reaction system by the spin-trapping method [18]. Specifically, 20 μl of a sample solution was mixed with 30 μl of 5 mM HPX, after which 20 μl of 5.5 mM diethylenetriaminepentaacetic acid (DTPA), 10 μl of 9 M DMPO, and 20 μl of 0.4 U/ml XO solution were added to the reaction solution in a test tube. The measurement was taken immediately after quickly stirring the mixture. A 200-μl aliquot of the mixture was placed into a flat cell.

2.7. *MTT cell viability assay*

The MTT [3-(4,5-dimethylthiazol-2-yl)-2,5-diphenyl tetrazolium bromide] assay was described by Hansen et al. [19] to test the cytotoxicity of reagents and cell viability. Cells (5000 cells per well) were grown on a 96-well plate supplemented with MEM medium (with 1% FBS) for 24 h. Cells were treated with aggregated $A\beta_{25-35}$ (15 μM), and the viability was determined by the reduction of MTT. For determining the protective effects

of coumarins on Aβ-induced neurotoxicity, Neuro-2A cells were co-treated with $A\beta_{25-35}$ (15 μM) for 24 h in the presence of coumarins (3.0 μM). An MTT stock solution (5 mg of MTT/ml of phosphate-buffered saline; PBS) was added to growing cultures (at a final concentration of 0.5 mg/ml). The OD was measured with a spectrophotometer (Thermo Varioskan Flash, Vantaa, Finland) at 560 nm. A blank with DMSO alone was measured and subtracted from all values.

2.8. Measurements of intracellular ROS

Levels of cellular oxidative stress were measured using the fluorescent probe, dihydrorhodamine 123 (DHR123), as described previously [20]. The DHR123 dye enters mitochondria and fluoresces when oxidized by ROS. After treatment with 15 μM of the $A\beta_{25-35}$ fragment or co-treatment with esculetin (3.0 μM) for 24 h, cells were stained with 10 μM

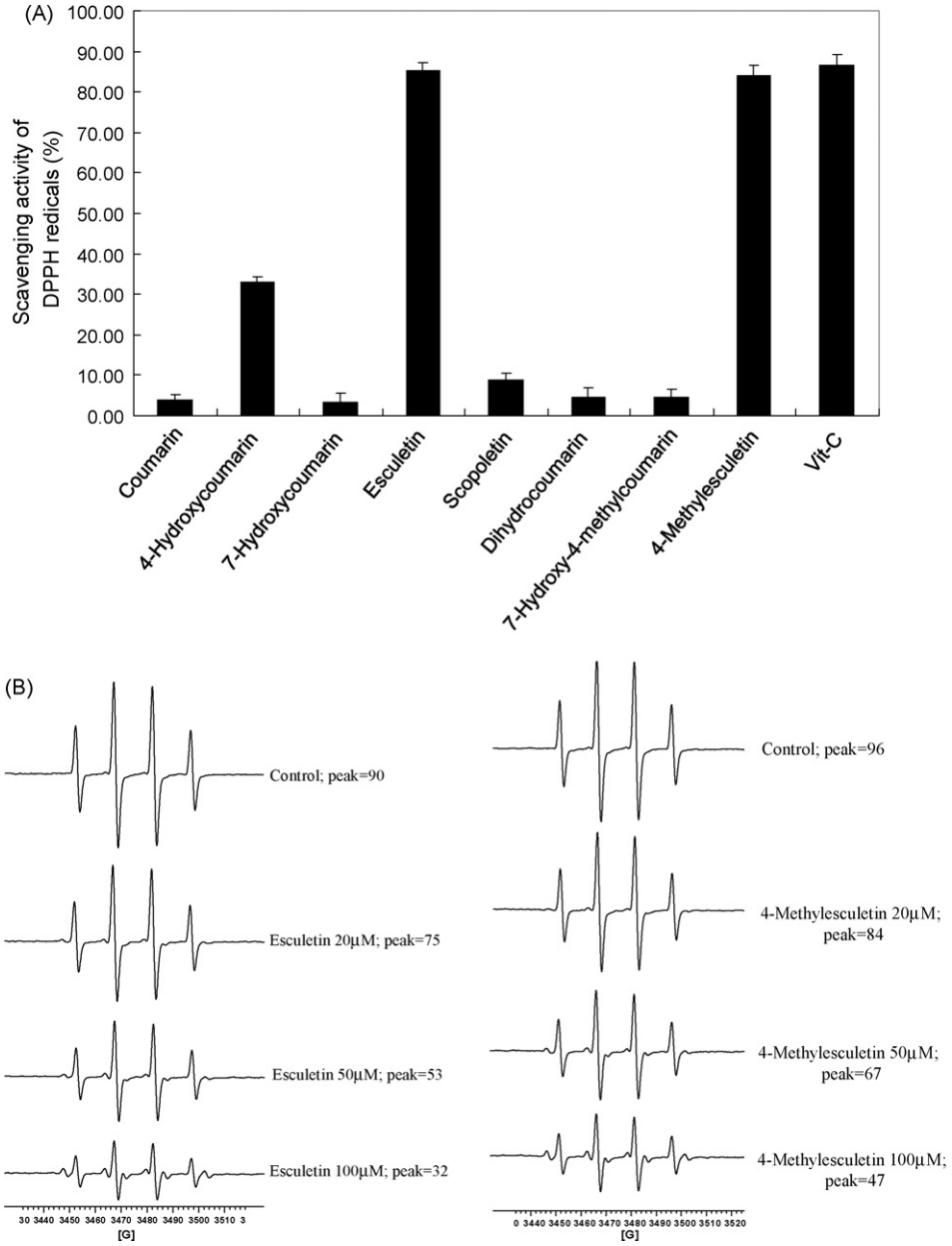

Fig. 2 – Antioxidative activities of coumarins on the DPPH radical and in the electron spin resonance (ESR) spectrum. (A) Effect of coumarin derivatives on the DPPH radical. The reaction mixtures containing 250 μM DPPH were incubated for 90 min at room temperature, after which the absorbance of the remaining DPPH was determined colorimetrically at 517 nm. The scavenging activity of coumarins (100 μM) was measured as the decrease in absorbance of DPPH expressed as a percentage of the absorbance of a control DPPH solution without coumarins. (B) Effect of esculetin and 4-methylesculetin on DMPO–OH formation. ESR spectra of the DMPO–OH signal obtained from the Fenton reaction system with various concentrations of esculetin (left panel) and 4-methylesculetin (right panel). Reaction mixtures contained 60 mM DMPO, 50 μM Fe(II), and 2 mM H_2O_2 (control) or various concentration (20, 50, and 100 μM) of the respective test compounds.

DHR123 for 30 min, and washed with PBS. Cells were imaged using a confocal microscope (Leica TCS SP5, Bensheim, Germany). Cells were located under bright-field optics and then scanned once with the laser (488 nm for excitation and 510 nm for emission).

3. Results

3.1. Antioxidative activities of coumarins

The extents of inhibition of DPPH– and DMPO–OH by the various test compounds were assessed to determine their antioxidant activities. Fig. 2A shows that esculetin and 4-methylesculetin were the two most potent agents in reducing DPPH radicals (with IC_{50} values of 5.42, and 5.91 μM, respectively, compared to ascorbic acid with an IC_{50} value of 9.95 μM) among the coumarins tested. 4-Hydroxylcoumarine displayed a less-potent effect with an IC_{50} value of 79.76 μM. Other selected coumarins had no significant effect in scavenging DPPH radicals.

ESR in combination with spin trapping techniques was utilized to further verify that the tested compounds possess the ability to scavenge hydroxyl radicals, and the results are shown in Fig. 1B. DMPO is the spin trapping reagent that reacts with hydroxyl radicals to generate the spin resonance signal, and this spin resonance signal can be quantified with ESR. The hydroxyl radical scavenger competes with DMPO for hydroxyl radicals; thus, the ESR signal will diminish. In the absence of an antioxidant, 2 mM of H_2O_2 and 50 μM of $FeSO_4$ generated an ESR signal with a peak height of 90, but under the same conditions, the peak heights of ESR signals were reduced to 32 in the presence of 100 μM esculetin (Fig. 2B, left panel). The IC_{50} (determined as the chemical concentration to reduce 50% of the peak height without the antioxidant) of esculetin was 72.83 μM, while that of 4-methylesculetin was 94.84 μM (Fig. 2B, right panel). The results were combined with prior results of the DPPH radical experiments, which suggested that esculetin and 4-methylesculetin are the two most effective radical scavengers among the tested coumarins.

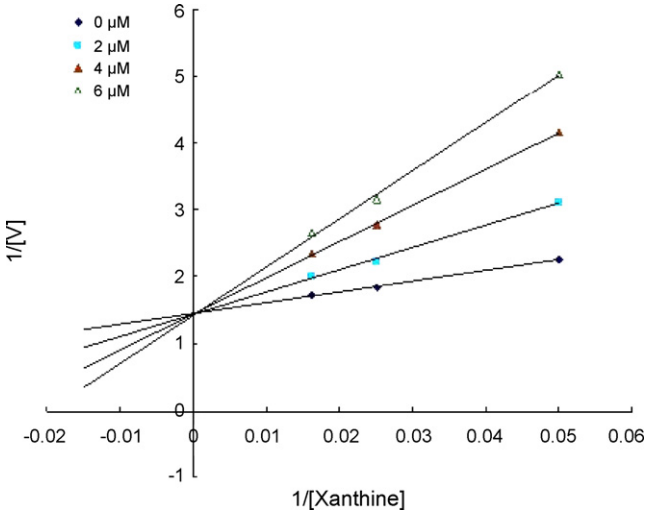

Fig. 3 – Kinetic assays of xanthine oxidase inhibition by esculetin. A Lineweaver–Burk double-reciprocal plot was constructed for the inhibition of xanthine oxidase by esculetin. The plot is expressed as 1/velocity vs. 1/xanthine (μM^{-1}) without or with an inhibitor in the reaction solution.

3.2. Competitive inhibition of XO by coumarins

The xanthine/XO (X/XO) reaction is an important biological source of ROS generators, and this reaction is known to be involved in many pathological processes. An inhibitor of XO has the potential to be a therapeutic agent for hyperuricemia and ROS-induced diseases. Allopurinol, a potent inhibitor of XO, is clinically used for gout treatment to prevent urate from accumulating in joints. XO has been reported to be inhibited by coumarins. Since the compounds tested herein are structural analogues of coumarins, we were also interested in studying the effects of these compounds on XO activities. Thus, we assayed the test compounds with XO, and the results were analyzed by Lineweaver–Burk plots. The Lineweaver–Burk plot revealed that esculetin competitively inhibited XO (Fig. 3) with an IC_{50} of 10.84 μM compared to an IC_{50} of 1.07 μM for allopurinol (Table 1). 4-Methylesculetin and 4-hydroxycoumarins were also competitive inhibitors with IC_{50} values of 75.79 and 78.13 μM, respectively. In contrast, coumarin, dihydrocoumarin, 7-hydroxycoumarin, scopoletin, and 7-hydroxy-4-methylcoumarin showed lower inhibitory activities (IC_{50} values of >100 μM) in this assay. Esculetin was the most potent inhibitor against XO among the tested compounds. These results indicated that all determined coumarin analogues were competitive inhibitors (Suppl. Fig. 1) of XO and they inhibited XO activities through a substrate binding blockade.

3.3. 3D modeling of the docking of coumarin derivatives on XO

We were interested in visualizing the effects of coumarins on XO in order to gain insights into the observed activities and elucidate the SARs; a 3D molecular model was created to evaluate the docking of selected compounds on XO. From prior kinetic assays, we learned that the test compounds were competitive inhibitors; therefore, we focused coumarin dockings on the active site, the molybdopterin domain of XO. All coumarins bind to the molybdopterin domain of XO, which forms several hydrogen bonds with the polypeptide residues. The carbonyl closely interacts with the guanidinium group of Arg880. The O atom of the pyrone ring forms hydrogen bonds with the hydroxyl side chain of Thr1010. Esculetin (Fig. 4A) and 4-methylesculetin (Fig. 4B) exhibited potent affinities toward the molybdopterin domain which is due to an interaction of the 6-hydroxyl with the E802 residue of XO. Methyl substitution of the 6-hydroxyl group of esculetin hampered the interaction with the E802 residue resulting in lower XO-inhibition activity of scopoletin (Fig. 4C). The 7-hydroxyl group forms a hydrogen bond with the H atom of the residue S876 (Fig. 4D). Coumarin (Suppl. Fig. 2A) and dihydrocoumarin (Suppl. Fig. 2B), both of which lack a hydroxyl group connected to the benzene ring, displayed a very low affinities to the

Table 1 – Inhibition of xanthine oxidase by coumarins

Compound	Inhibition (%)[a]	IC_{50} (μM)[b]	Inhibition type
Coumarin	1.59 ± 5.61	>100	ND
4-Hydroxycoumarin	37.18 ± 3.80	78.13 ± 3.11	Competitive
7-Hydroxycoumarin	8.67 ± 3.05	>100	Competitive
Esculetin	83.44 ± 2.76	10.84 ± 0.14	Competitive
Scopoletin	4.55 ± 3.46	>100	Competitive
Dihydrocoumarin	5.32 ± 3.90	>100	ND
7-Hydroxy-4-methylcoumarin	4.65 ± 2.93	>100	Competitive
4-Methylesculetin	37.35 ± 2.20	75.79 ± 1.98	Competitive
Allopurinol	99.43 ± 2.23	1.07 ± 0.01	Competitive

ND: not determined.
[a] The percent (%) inhibition was calculated according to the formula: [(product formation of the uninhibited control – product formation of 50 μM coumarin)/(product formation of the uninhibited control)] × 100%.
[b] The IC_{50} value was determined as the chemical concentration which inhibited 50% of the enzyme activity with 3 U/l xanthine oxidase and 50 μM xanthine as substrate.

enzyme. The interaction between 4-hydroxyl and a water molecule was important for coumarin binding (Suppl. Fig. 2C). The docking interaction energies of various test compounds (Suppl. Table 1) reflected the affinities and were consistent with the IC_{50} values to a certain extent.

3.4. *Total activities of reducing ROS formation and ROS scavenging by coumarins in the hypoxanthine/XO reaction*

In addition to possessing ROS-scavenging activity, coumarins also inhibit XO activity leading to a reduction in ROS

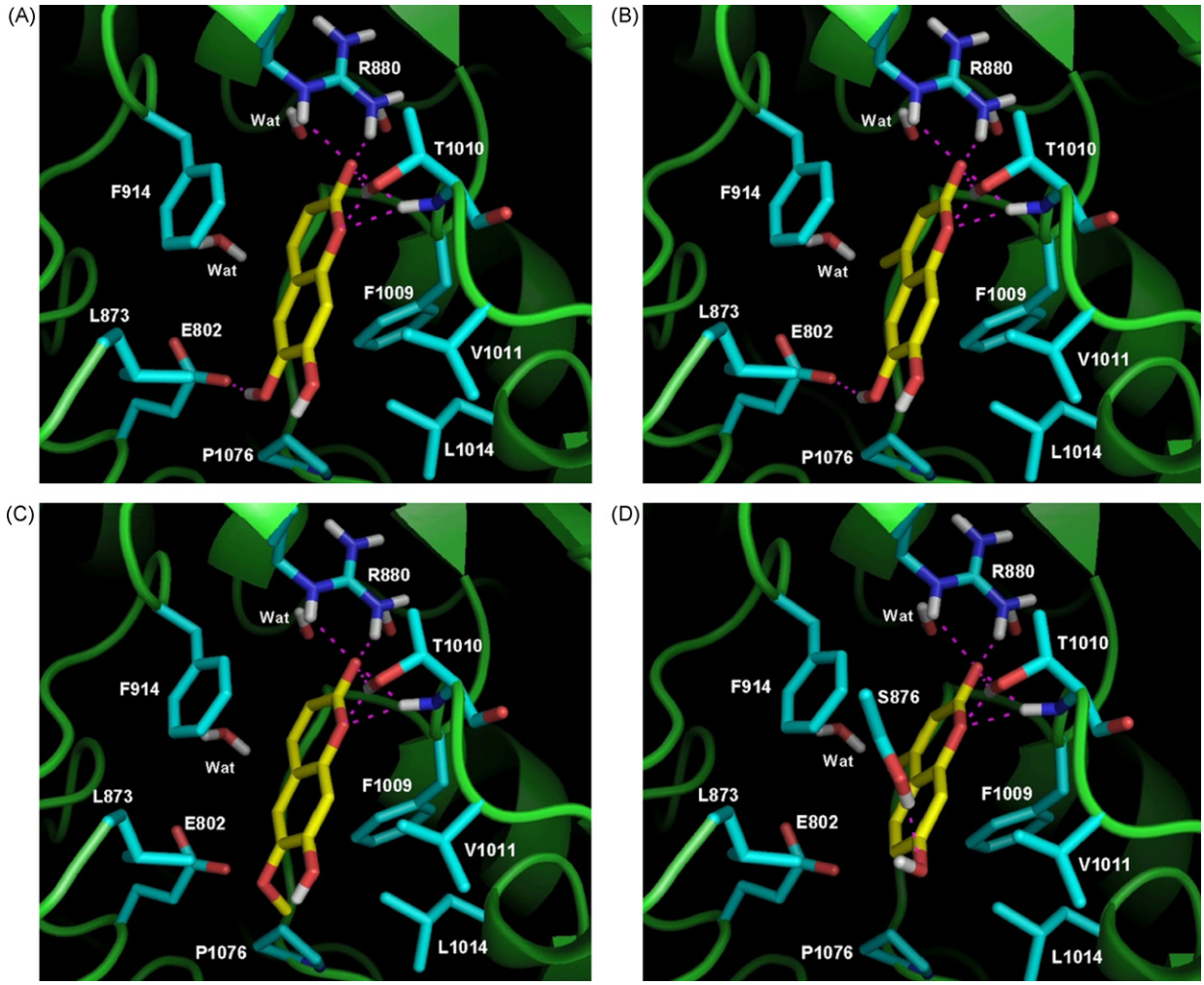

Fig. 4 – Molecular models of the binding of coumarins to the active site of xanthine oxidase. A three-dimensional model of the coumarins: (A) esculetin, (B) 4-methylesculetin, (C) scopoletin, and (D) 4-methyl-7-hydroxycoumarin.

Table 2 – Total activities of reduced ROS formation and ROS scavenging by coumarins in the hypoxanthine/xanthine oxidase reaction using electron spin resonance (ESR) combined with the DMPO trapping assay

Compound	Inhibition of the DMPO–OOH signals (%)
Coumarin	10.88 ± 0.81
4-Hydroxycoumarin	70.9 ± 1.73
7-Hydroxycoumarin	15.14 ± 1.97
Esculetin	89.16 ± 0.91
Scopoletin	37.48 ± 5.45
Dihydrocoumarin	20.52 ± 8.89
7-Hydroxy-4-methylcoumarin	32.64 ± 16.51
4-Methylesculetin	81.18 ± 1.09
Allopurinol	46.16 ± 2.83

The abilities of 200 μM coumarins or allopurinol to scavenge superoxide radicals produced from 0.6 mM hypoxanthine and 0.0018 U XO were measured by ESR spectroscopy as described in Section 2. Data represented as the mean ± S.D., $n = 4$. The percent (%) inhibition was calculated according to the formula: [(peak height of the control − peak height of coumarin)/(peak height of the control)] × 100%.

formation. From above experimental results, esculetin was the most potent inhibitor of XO and ROS scavenger among the tested compounds. We used ESR combined with the DMPO trapping assay with xanthine/hypoxanthine in the presence or absence of coumarins to evaluate their total activities for ROS scavenging and reducing ROS formation, and the results are shown in Table 2. Esculetin (89.16% inhibition) was the most potent agent competing with DMPO on ESR signals compared with 4-methylesculetin and allopurinol (81.18 and 46.16% inhibition, respectively). Supplemental Fig. 3 shows the dose-dependent manner of suppression of the ESR peak heights with esculetin and 4-methylesculetin treatments. Scopoletin (37.48% inhibition) and 7-hydroxy-4-methylcoumarin (32.64% inhibition) displayed weaker effects, whereas dihydrocoumarin (20.52% inhibition), 7-hydroxycoumarin (15.14% inhibition), coumarin (10.88% inhibition), and 4-hydroxycoumarin (7.09% inhibition) exhibited substantially weaker effects.

3.5. *Coumarins inhibited ROS-associated Aβ-induced cytotoxicity in living cells*

The β-amyloid peptide (Aβ) is a cytotoxic agent against neurons cells. The formation of Aβ is closely correlated with the intracellular oxidative stress which causes the peroxidation of membrane lipids and ultimately leads to cell death. Since the above results showed that coumarins are effective agents in reducing oxidative stress, we further evaluated the rescue effects of coumarins on Neuro-2A cells under oxidative stress. Neuro-2A cells were treated with $A\beta_{25-35}$ (15 μM) for 24 h in the presence or absence of coumarins, and the results of cell viability were determined by measuring the metabolism of the tetrazolium substrate, MTT as shown in Fig. 5A. Cell viability upon Aβ treatment for 24 h was about 50%, which was rescued by esculetin (3.0 μM) to about 70%. The protective effects were calculated according to the reduced cytotoxicity with coumarin treatments (3.0 μM). Esculetin was more potent than other coumarins at a concentration of 3.0 μM. The order of the protective effects for the tested coumarins was esculetin > 4-methylesculetin ≒ scopoletin > coumarin ≒ 4-hydroxycoumarin, 7-hydroxycoumarin, dihydrocoumarin, and 7-hydroxy-4-methylcoumarin (Fig. 5A). In an attempt to identify coumarin inhibition on ROS-associated cytotoxicity upon Aβ-treatment, cells were incubated with DHR123. This nonfluorescent compound selectively accumulates in mitochondria, where it can be oxidized by mitochondria-derived ROS to a fluorescent rhodamine derivative. As demonstrated in Fig. 5B, Aβ-treatment (b) resulted in a significant increase in DHR123 fluorescence compared to the untreated control (a), while the fluorescence intensity was reduced by co-treatment of Aβ and esculetin (c). These results show that esculetin was effective in reducing the Aβ-induced rise in ROS levels.

4. Discussion

Our study demonstrates that selected coumarins are competitive inhibitors of XO, and they are also potent superoxide-suppressive agents. Natural and synthetic coumarins have been determined to have antioxidant, anti-inflammatory, anticoagulation, and anticancer activities. In various *in vivo* experiments, rats with ameliorated hepatotoxicity treated with coumarins showed a significant reduction in oxidative stress [21]. Our results in Fig. 2 demonstrate that the chemical structures of both esculetin and 4-methylesculetin bear two hydroxyl moieties on the benzene rings, and these were the two most effective radical scavengers among the tested compounds. All other selected coumarins only carried one hydroxyl group or no free hydroxyl group in their chemical structure. This suggests that the radical-scavenging effects of coumarins are correlated with the number of hydroxyl groups. A similar correlation was also reported for flavonoids [22] and cinnamic acids [23]. Methoxy-substituted scopoletin exhibited lower effectiveness in scavenging radicals compared to esculetin. The result is consistent with a previous report that the scavenging capacity was higher for caffeic acid bearing OH groups than the methoxy-substituted derivatives [24]. We suggest that the resonance structures of the radical derived from esculetin and 4-methylesculetin are especially stable because of the *ortho*-quinone form of the resonance structure. There are more resonance structures in esculetin and 4-methylesculetin than in the other coumarins tested.

In general, orally administered phenolic compounds undergo hydroxylation and/or glucuronide and sulfate conjugation primarily by intestinal microflora and secondarily in the liver and other tissues. It is well known that phenolic methoxyl groups of coumarins are demethylated in the liver [25]. It has been reported that consuming a diet containing coumarin affects aflatoxin B1 metabolism which enhances aflatoxin B1 detoxification through the suppression of P450 enzyme activity in the liver and enhancement of GST activity in the intestine [26]. The flavonoid silybin contains five hydroxyl groups and has been shown to have hepatoprotective properties as well as anticarcinogenic effects in animal models, and this may be related to its ability to inhibit some P450 isoforms, whereas flavonoids without hydroxyl groups seem to stimulate P450 activity [27]. Esculetin, which can reduce tissue edema and inflammation, has been reported to

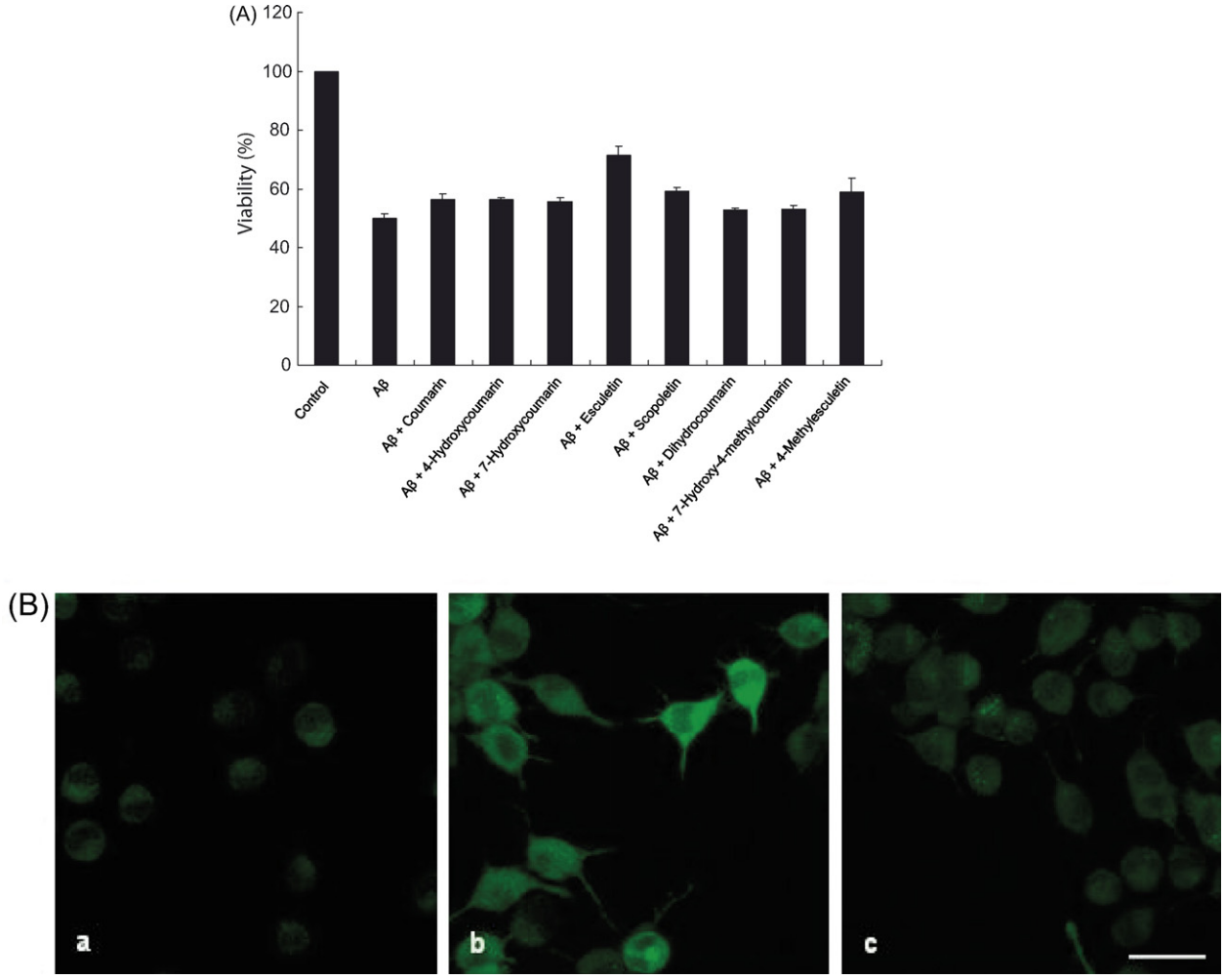

Fig. 5 – Coumarin derivatives inhibited Aβ-induced cytotoxicity and ROS production in living cells. (A) Coumarins protected Neuro-2A cells from Aβ-induced cytotoxicity. Neuro-2A cells were treated with the $A\beta_{25-35}$ fragment for 24 h in the presence or absence of various coumarins. Cell viability was measured by the MTT assay. Neuro-2A cells without Aβ treatment served as a control. (B) ROS amounts in a confocal image of Aβ-treated Neuro-2A cells with DHR123 fluorescence. (a) Control, (b) at 24 h following 15 μM Aβ addition, and (c) at 24 h following 15 μM Aβ with 3.0 μM esculetin addition. Bars = 20 μm.

have multiple biological activities [8]. The metabolic roles of hydroxyl moieties on coumarins remain to be further investigated.

The crystalline structure of XO was first reported by Enroth et al. [7]. Chang et al. reported that phenylpropanoids [24] bind to the active site of XO and prevent substrate entrance toward the Mo-pt center. The chemical structures of both esculetin and 4-methylesculetin are comprised of two hydroxyl groups on the benzene moiety which were more effective in scavenging radicals compared to other selective compounds, and they were also the most potent inhibitors against XO. In our enzyme kinetic assay experiments, we found that esculetin was a more-potent inhibitor than 4-methylesculetin. We speculated according to the results of the molecular docking experiments that the additional methyl group of 4-methylesculetin generates a repulsive force with a water molecule in XO and leads to 7-hydroxyl apart from S876. We learned from the molecular docking results that both esculetin and 4-methylesculetin interacted favorably with the active site of XO through the formation of a hydrogen bond by the 6-hydroxyl group of the inhibitors with the Glu802 residue. The chemical structure of scopoletin is similar to that of esculetin with the only difference being a methoxy substituted for 6-hydroxyl, and this modification of the chemical structure results in diminished inhibition potency of scopoletin against XO. This further implies that the H atom of the 6-hydroxyl plays a more important role than the O atom.

The coumarins tested herein were potent ROS scavengers, and they were also effective inhibitors against XO's reduction of ROS production. Intracellular ROS production is associated with a number of cellular events including activation of NADPH oxidase, XO, and the cellular mitochondrial respiratory chain [28]. ROS thus formed are potent activators of inflammatory signal transduction pathways, such as the MAPK cascade which triggers a series of responses in which IκB is phosphorylated to free NF-κB from IκB inhibition [29,30].

Esculetin with its potent antioxidant actions may suppress NF-κB activation, and lead to suppression of COX-2 expressions. In the *in vitro* experiment, esculetin was the most potent agent inhibiting XO activity and scavenging ROS (Table 2). The fact that esculetin exhibits more-potent effects in reducing ROS-associated Aβ-toxicity in neuron cells reflects the conclusion made in the *in vitro* experiments. Because there are numerous ROS sources in addition to XO, esculetin inhibits not only XO but can also block NADPH oxidase and maintain mitochondrial function to reduce ROS amounts, whereas allopurinol has only a single role of xanthine oxidase inhibition.

Acknowledgements

This study was supported by grants from the National Science Council (NSC96-2113-M-038-001) and Taipei Medical University Hospital (94TMU-TMUH-01).

Appendix A. Supplementary data

Supplementary data associated with this article can be found, in the online version, at doi:10.1016/j.bcp.2007.11.023.

REFERENCES

[1] Berg D, Youdim MB, Riederer P. Redox imbalance. Cell Tissue Res 2004;318:201–13.
[2] Mircescu G. Oxidative stress: an accomplice to uremic toxicity? J Ren Nutr 2006;16:194–8.
[3] Perez-Ortiz JM, Tranque P, Burgos M, Vaquero CF, Llopis J. Glitazones induce astroglioma cell death by releasing reactive oxygen species from mitochondria: modulation of cytotoxicity by nitric oxide. Mol Pharmacol 2007;72:407–17.
[4] Nakai K, Kadiiska MB, Jiang JJ, Stadler K, Mason RP. Free-radical production requires both inducible nitric oxide synthase and xanthine oxidase in LPS-treated skin. Proc Natl Acad Sci USA 2006;103:4616–21.
[5] Schroder K, Vecchione C, Jung O, Schreiber JG, Shiri-Sverdlov R, van Gorp PJ, et al. Xanthine oxidase inhibitor tungsten prevents the development of atherosclerosis in ApoE knockout mice fed a Western-type diet. Free Radic Biol Med 2006;41:1353–60.
[6] Okamoto K, Matsumoto K, Hille R, Eger BT, Pai EF, Nishino T. The crystal structure of xanthine oxidoreductase during catalysis: implications for reaction mechanism and enzyme inhibition. Proc Natl Acad Sci USA 2004;101:7931–6.
[7] Enroth C, Eger BT, Okamoto K, Nishino T, Nishino T, Pai EF. Crystal structures of bovine milk xanthine dehydrogenase and xanthine oxidase: structure-based mechanism of conversion. Proc Natl Acad Sci USA 2000;97:10723–8.
[8] Fylaktakidou KC, Hadjipavlou-Litina DJ, Litinas KE, Nicolaides DN. Natural and synthetic coumarin derivatives with anti-inflammatory/antioxidant activities. Curr Pharm Des 2004;10:3813–33.
[9] Voora D, McLeod HL, Eby C, Gage BF. The pharmacogenetics of coumarin therapy. Pharmacogenomics 2005;6:503–13.
[10] Hatano T, Yasuhara T, Fukuda T, Noro T, Okuda T. Phenolic constituents of licorice. II. Structures of licopyranocoumarin, licoarylcoumarin and glisoflavone, and inhibitory effects of licorice phenolics on xanthine oxidase. Chem Pharm Bull (Tokyo) 1989;37:3005–9.
[11] Chang WS, Chiang HC. Structure–activity relationship of coumarins in xanthine oxidase inhibition. Anticancer Res 1995;15:1969–73.
[12] Ferrari AM, Sgobba M, Gamberini MC, Rastelli G. Relationship between quantum-chemical descriptors of proton dissociation and experimental acidity constants of various hydroxylated coumarins. Identification of the biologically active species for xanthine oxidase inhibition. Eur J Med Chem 2007;42:1028–31.
[13] Chen C, Tang HR, Sutcliffe LH, Belton PS. Green tea polyphenols react with 1,1-diphenyl-2-picrylhydrazyl free radicals in the bilayer of liposomes: direct evidence from electron spin resonance studies. J Agric Food Chem 2000;48:5710–4.
[14] Lin CM, Chen CT, Lee HH, Lin JK. Prevention of cellular ROS damage by isovitexin and related flavonoids. Planta Med 2002;68:365–7.
[15] Morris GM, Goodsell DS, Halliday RS, Huey R, Hart WE, Belew RK, et al. Automated docking using a Lamarckian genetic algorithm and empirical binding free energy function. J Comput Chem 1998;19:1639–62.
[16] Gasteiger J, Marsili M. Iterative partial equalization of orbital electronegativity: a rapid access to atomic charges. Tetrahedron 1980;36:3219–28.
[17] Lin CM, Huang ST, Lee FW, Kuo HS, Lin MH. 6-Acyl-4-aryl/alkyl-5,7-dihydroxy-coumarins as anti-inflammatory agents. Bioorg Med Chem 2006;14:4402–9.
[18] Kurihara H, Fukami H, Toyoda Y, Kageyama N, Tsuruoka N, Shibata H, et al. Inhibitory effect of oolong tea on the oxidative state of low density lipoprotein (LDL). Biol Pharm Bull 2003;26:739–42.
[19] Hansen MB, Nielsen SE, Berg K. Re-examination and further development of a precise and rapid dye method for measuring cell growth/cell kill. J Immunol Meth 1989;119:203–10.
[20] Keller JN, Guo Q, Holtsberg FW, Bruce-Keller AJ, Mattson MP. Increased sensitivity to mitochondrial toxin-induced apoptosis in neural cells expressing mutant presenilin-1 is linked to perturbed calcium homeostasis and enhanced oxyradical production. J Neurosci 1998;18:4439–50.
[21] Lin WL, Wang CJ, Tsai YY, Liu CL, Hwang JM, Tseng TH. Inhibitory effect of esculetin on oxidative damage induced by *t*-butyl hydroperoxide in rat liver. Arch Toxicol 2000;74:467–72.
[22] Heim KE, Tagliaferro AR, Bobilya DJ. Flavonoid antioxidants: chemistry, metabolism and structure–activity relationships. J Nutr Biochem 2002;13:572–84.
[23] Siquet C, Paiva-Martins F, Lima JL, Reis S, Borges F. Antioxidant profile of dihydroxy- and trihydroxyphenolic acids: a structure–activity relationship study. Free Radic Res 2006;40:433–42.
[24] Chang YC, Lee FW, Chen CS, Huang ST, Tsai SH, Huang SH, et al. Structure–activity relationship of C6-C3 phenylpropanoids on xanthine oxidase-inhibiting and free radical-scavenging activities. Free Radic Biol Med 2007;43:1541–51.
[25] Mennes WC, Luijckx NB, Wortelboer HM, Noordhoek J, Blaauboer BJ. Differences in the effects of model inducers of cytochrome P450 on the biotransformation of scoparone in rat and hamster liver. Arch Toxicol 1993;67:92–7.
[26] Tulayakul P, Dong KS, Li JY, Manabe N, Kumagai S. The effect of feeding piglets with the diet containing green tea extracts or coumarin on in vitro metabolism of aflatoxin B1 by their tissues. Toxicon 2007;50:339–48.
[27] Sridar C, Goosen TC, Kent UM, Williams JA, Hollenberg PF. Silybin inactivates cytochromes P450 3A4 and 2C9 and

inhibits major hepatic glucuronosyltransferases. Drug Metab Dispos 2004;32:587–94.
[28] Abramov AY, Scorziello A, Duchen MR. Three distinct mechanisms generate oxygen free radicals in neurons and contribute to cell death during anoxia and reoxygenation. J Neurosci 2007;27:1129–38.
[29] Choi HB, Ryu JK, Kim SU, McLarnon JG. Modulation of the purinergic P2X7 receptor attenuates lipopolysaccharide-mediated microglial activation and neuronal damage in inflamed brain. J Neurosci 2007;27:4957–68.
[30] Longpre F, Garneau P, Christen Y, Ramassamy C. Protection by EGb 761 against beta-amyloid-induced neurotoxicity: involvement of NF-kappaB, SIRT1, and MAPKs pathways and inhibition of amyloid fibril formation. Free Radic Biol Med 2006;41:1781–94.